DOI: 10.31319/2519-8106.2(49)2023.293108
УДК 621.736: 539.213.28

Sereda Borys[1], doctor of technical sciences, professor, Head Department of automobiles and automotive industry
Середа Б.П., доктор технічних наук, професор, завідувач кафедри автомобілів та автомобільне господарство
ORCID: 0000-0002-9518-381X
e-mail: seredabp@ukr.net

Baskevich Oleksandr[2], Candidate of Physico-mathematical Sciences, Associate Professor, Senior Researcher in the Research Unit
Баскевич О.С., кандидат фізико-математичних наук, старший науковий співробітник НДЧ
ORCID: 0000-0002-3227-5637

Gulivets Alexey[3], Candidate of Physical and Mathematical Sciences, Associate Professor
Гуливець О.М., кандидат фізико-математичних наук, доцент
ORCID: 0000-0003-3410-9605

Udod Andrey[4], Director, Chief designer
Удод А.М., директор, головний конструктор
ORCID: 0000-0001-8029-4878

[1]Dniprovsky State Technical University, Kamianske
Дніпровський державний технічний університет, м. Кам'янське
[2]Ukrainian State University of Chemical Technology, Dnipro
Український державний хіміко-технологічний університет, м. Дніпро
[3]Ukrainian State University of Science and Technology, Dnipro
Український державний університет науки і техніки, м. Дніпро
[4]Limited Liability Company "Ukrainian Research Design and Technology Institute of Elastomeric Materials and Products, Dnipro
Товариство з обмеженою відповідальністю «Український науково-дослідний конструкторсько-технологічний інститут еластомерних матеріалів і виробів», м. Дніпро

SIMULATION OF THE FORMATION OF PROTECTIVE COATINGS USING THE RADIAL DISTRIBUTION FUNCTION OF ATOMS

МОДЕЛЮВАННЯ ФОРМУВАННЯ ЗАХИСНИХ ПОКРИТТІВ ЗА ДОПОМОГОЮ ФУНКЦІЇ РАДІАЛЬНОГО РОЗПОДІЛУ АТОМІВ

Studies of the structural factors of alloys, carried out using wide-angle and small-angle X-ray studies, allowed us to identify general patterns for various alloys. The use of apodization of the Fourier distribution of X-ray diffraction (XRD) contributes to the leveling of the effect of the break in the experimental intensity curve and facilitates close-order modeling. It was established that the height of the main peak of the structural factor decreases, and the position slightly shifts towards larger angles when the arrangement of alloys increases. The second maxima of the structural factor have an asymmetric shape, which varies depending on the conditions for obtaining the alloys. As the amount of phosphorus in the alloys decreases, the relief and height of the peaks increase. It was found that the diversity of the close order of the alloys is related to the deposition conditions, in particular, to a large value of the overvoltage at the cathode and the penetration of phosphorus atoms into the structure of the alloys. The obtained modeling results allow us to establish the conditions for the formation of close order in alloys and expand our understanding of the structural features of materials.

***Keywords**: Wide-angle X-ray analysis, apodization of the Fourier distribution of X-ray diffraction, penetration of atoms, deposition, ordering of alloys.*

Дослідження структурних факторів сплавів, проведені з використанням ширококутового та малокутового рентгенівських досліджень, дозволили виявити загальні закономірності для різних сплавів. Використання аподизації Фур'є-розкладу рентгенівської дифракції (ФРРА) сприяє нівелюванню ефекту обриву експериментальної кривої інтенсивності та полегшує моделювання близького порядку. Встановлено, що висота головного піка структурного фактору зменшується, а положення незначно зміщується в бік більших кутів при збільшенні порядкування сплавів. Другі максимуми структурного фактору мають асиметричну форму, яка змінюється в залежності від умов отримання сплавів. Зі зменшенням кількості фосфору в сплавах рельєфність і висота піків зростають. Виявлено, що різноманітність близького порядку сплавів пов'язана з умовами осадження, зокрема з великим значенням перенапруги на катоді та проникненням в структуру сплавів атомів фосфору. Отримані результати моделювання дозволяють встановити умови формування близького порядку в сплавах та розширюють наше розуміння структурних особливостей матеріалів.

***Ключові слова**: ширококутовий рентгенівський аналіз, аподизації Фур'є-розкладу рентгенівської дифракції, проникнення атомів, осадження, порядкування сплавів.*

Problem's Formulation

The research problem is to consider the formation of amorphous transition metal alloys with phosphorus during electropulse deposition. The study of this process requires clarification of general patterns for different alloys and consideration of the influence of various factors, such as phosphorus concentration and deposition conditions. Determining the conditions for the formation of close-order alloys and their properties is key to further improving technologies for obtaining materials with improved physical and chemical characteristics. The search for optimal conditions for the synthesis of amorphous alloys opens up ways to improve their use in various industries.

Analysis of recent research and publications

Reliable curves of the radial distribution function of atoms (RDFA) are obtained by integrating the experimental structural factor from 0 to , which for disordered structures quickly dies out. Of course, if the experimental conditions are limited, the phenomenon of a break in the experimental intensity curves must be taken into account. Many works [2—5] have been devoted to the influence of the experimental intensity break on the FRRA.

Formulation of the study purpose

The aim of the study is to reveal the structural factors of alloys through the use of wide-angle and small-angle X-ray analysis. The study aims to investigate the general patterns for various alloys and determine the effect of FRPA apodization on the experimental intensity curves. In addition, the goal is to analyze changes in the height and position of the main structural factor peaks when ordering the alloys. The study of the difference in coordination numbers of amorphous alloys compared to crystalline cobalt is used to understand the peculiarities of their structure. The results of such a study can indicate the conditions for the formation of close order in alloys and reveal its relationship with the conditions of deposition and the presence of phosphorus atoms in the structure.

Presenting main material

Many studies have been devoted to the influence of the experimental intensity break on the XRD, which consider various manifestations of the Gibbs effect associated with the break of the upper integration limit in the Fourier transform [1]**:**

$$F(s) = s\left[a(s) - 1\right] = \int_0^\infty 4\pi \cdot x \sin(sx)dx\,, \tag{1}$$

This expression is valid for the range of values $s \in \left[0, s_m\right]$. The Fourier transform is valid for an infinite range of the definition of *F(s)*, represented by formula (1). If the upper bound of (1) is limited

to the maximum value of S_m,, then (1) should be multiplied by 2Sin(sr)/p and integrated over S in the interval $[0,S_m]$, taking into account that the pair function $c(r)=c(-r)$ is used:

$$\frac{2}{\pi}\int_0^{S_m} F(s)\sin(sr)ds = \frac{2}{\pi}\int_0^{\infty} 4\pi\cdot x[\rho(x)-\rho_0]dx\int_0^{S_m}\sin(sx)\sin(sr)ds =$$

$$= \int_{-\infty}^{\infty} 4\pi\cdot x[\rho(x)-\rho_0]\int_0^{S_m}\cos(s(r-x))ds = \int_{-\infty}^{\infty} 4\pi\cdot x[\rho(x)-\rho_0]\frac{\sin(s_m(r-x))}{r-x}dx\,. \qquad (2)$$

If in (2) we make a transformation:

$$\frac{1}{\pi}\int_{-\infty}^{\infty} 4\pi\cdot x\rho_0\frac{\sin(s_m(r-x))}{r-x}dx = 4\rho_0\int_{-\infty}^{\infty}(r-t)\frac{\sin(s_m t)}{t}dt = 4\pi\cdot r\rho_0\,, \qquad (3)$$

we get the equation:

$$G(r) = \int_{-\infty}^{\infty} 4\pi\cdot x\rho(x)\frac{\sin(s_m(r-x))}{r-x}dx = 4\pi\cdot r\rho_0 + \frac{2}{\pi}\int_{-\infty}^{\infty}F(s)\sin(sr)ds\ , \qquad (4)$$

where instead of the function $G(r)$ its convolution $\sin(s_m r)/r$. is used. To follow the main details of the Gibbs effect, we represent the FRRA as a set of α-Dirac functions:

$$G(r) = 4\pi\cdot r\rho(r) = \sum_k \frac{Z_k}{r_k}\delta(r-r_k)\,, \qquad (5)$$

where Zk are coordination numbers, rk are the radii of the corresponding coordination spheres.

This model describes the arrangement of atoms in crystals at temperatures close to absolute zero, when the width of individual peaks $G(r)$ is much smaller than the width of standard peaks $Sin(s_m r)/r$. For the apodized model, (5) follows from (4):

$$G(r) = \frac{1}{\pi}\sum_k \frac{Z_k}{r_k}\frac{\sin(s_m(r-r_k)}{r-r_k} = 4\pi\cdot r\rho_0 + \frac{2}{\pi}\int_0^{S_m}F(s)exp(-\tau\cdot s^2)\sin(sr)ds\,, \qquad (6)$$

The FRRA peaks obtained as a result of a break in the intensity curve have an integral width:

$$\delta S = \frac{\int_{-\infty}^{\infty}\frac{\sin(s_m(r-r_k)\cdot e^{-\tau\cdot S_m^2}}{r-r_k}dr}{s_m} = \frac{2arctg\left(\frac{S_m}{\tau}\right)}{s_m}\,, \qquad (7)$$

To determine the error Д$G(r)$ between the XRD of the amorphous $Ni_{86}P_{14}$, alloy calculated from the experimental structural factor and the XRD calculated from the approximated structural factor from S = 0 to 300 nm-1 using the Percus-Evick method [1], it was found that the main error is at values of R from 0 to 0.4 nm (Fig. 1).

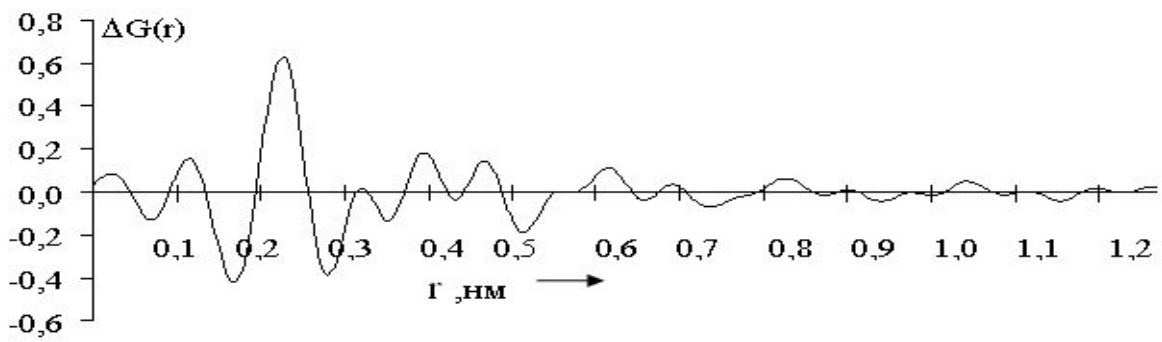

Fig. 1. Error in determining the FRRA $\Delta G(r)$ of $Ni_{86}P_{14}$, alloy caused by the break in the intensity curve S_2 =110 нм$^{-1}$

To eliminate the effect of the break, it is not enough to increase the upper integration limit in the right part of (6), which shows that oscillations of the FRRA wings are observed at any final value of S_m. However, increasing the upper limit of integration leads to an increase in the amplitude of oscillations, which is associated with errors in determining the structural factor.

To eliminate the Gibbs effect and the oscillating wings of peaks (sub-peaks), the apodization method is used. The appearance of oscillating wings is not related to the upper limit of integration on the right side of (6), but to the type of function that limits the function *F(s)* from the side of large values of *S*. For PM-M alloys, the best results are obtained when using an apodizing function [1]:

$$\varphi(s) = \exp(-\tau \cdot s^2), \quad \tau > 0, \tag{8}$$

for which the FRRA was obtained:

$$G(r) = 4\pi \cdot r\rho_0 + \frac{2}{\pi}\int_0^{S_m} F(s)e^{-\tau s^2}\sin(sr)ds, \tag{9}$$

which is valid if the equality holds for it with a sufficient degree of accuracy:

$$\int_0^{S_m} e^{-\tau \cdot s^2}\cos(sr)ds \cong \frac{1}{\sqrt{4\pi\tau}}\exp\left[-\frac{r^2}{4\tau}\right]. \tag{10}$$

The apodizing function (8) leads to smooth wings of the FRRA peaks and suppresses the FRRA error associated with the structural factor break (Fig. 2). To determine the required apodization coefficient, it is necessary to calculate the FRRA using formula (9), using different τ so as to eliminate false maxima, including those in the range of 0—0.2 nm, and minimize the distortion of the FRRA. Fig. 2 shows the curves of the effect of the apodization coefficient on the errors in determining the FRRA of the amorphous $Ni_{86}P_{14}$, alloy associated with the break in the structural factor, which shows that when using the apodization coefficient τ = 0.02, the errors associated with the break effect almost disappear. In practice, structure modeling is started when the apodization factor is experimentally found to have the least impact on the FRRA.

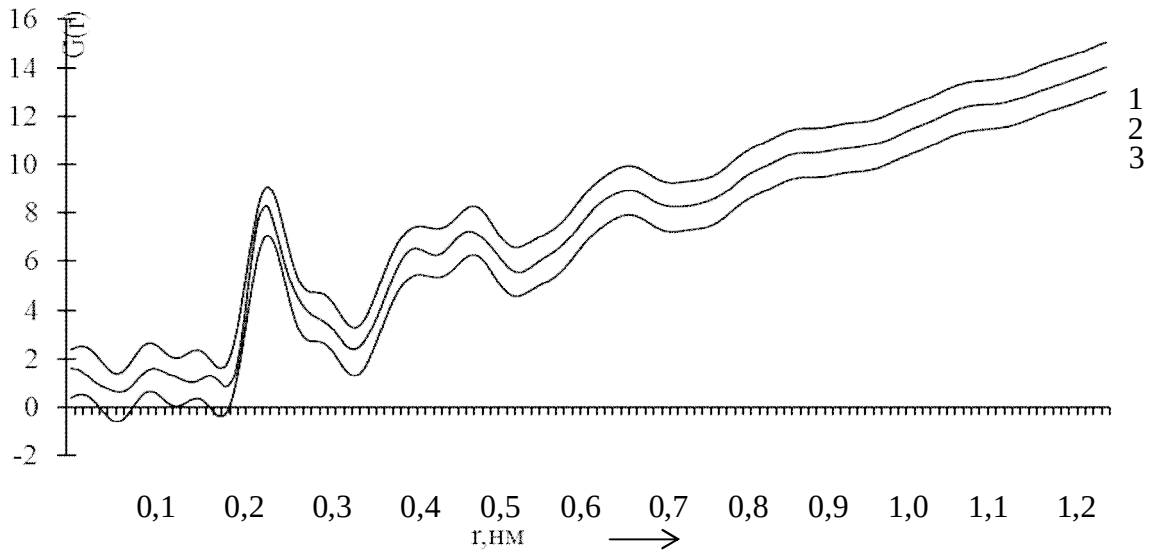

Fig. 2. Effect of the apodization coefficient on the XRD of the amorphous $Ni_{86}P_{14}$ alloy: 1 — ф=0, 2 — ф=0,01, 3 — ф=0,02

To estimate the size of the inhomogeneity regions, we used the Guinier approximation for the small-angle X-ray scattering (SAS) intensity, which made it possible to calculate the radii of inertia of the SAS and the size of the inhomogeneities. Fig. 3—5 show the dependence of the SERS intensity of Ni-P, Fe-P, and Co-P alloys on the phosphorus content, which showed that the shape of the diffraction

curves describes the shape of inhomogeneities close to the spherical shape, and with an increase in the crystalline fraction in the alloys, the SERS intensity increases. For Ni-P alloys with a decrease in phosphorus content from 16 to 10 at. %, the radius of inertia increases from 2.8 to 7.1 nm, for Fe-P alloys with a decrease in phosphorus composition from 17 to 13 at. % the radius of inertia increases from 2.8 to 7.5 nm, and for Co-P alloys with a decrease in phosphorus content from 17 to 10 at. %, the radius of inertia increases from 2.1 to 6.5 nm.

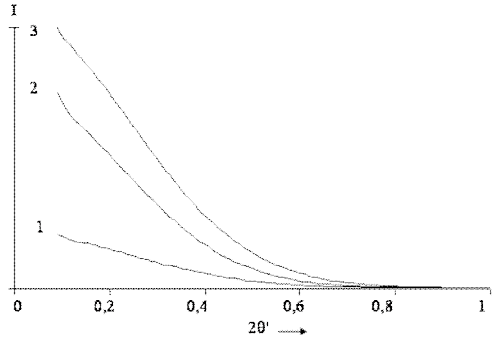

Fig. 3. Intensity of MCRR by amorphous alloys: 1 – $Ni_{86}P_{14}$;2 – $Ni_{88}P_{12}$; 3 – $Ni_{90}P_{10}$. Cu-*Ka* radiation

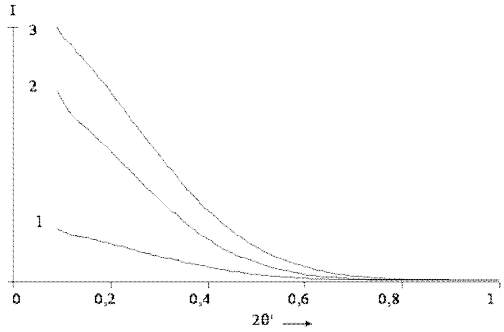

Fig. 4. Intensity of MCRR by amorphous alloys: 1 — $Fe_{83}P_{17}$;2 — $Fe_{85}P_{15}$; 3 — $Fe_{87}P_{13}$. Cu-Ka radiation

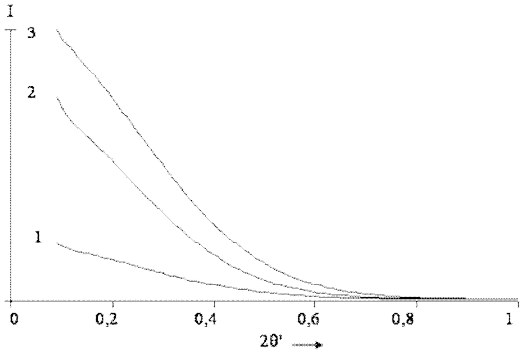

Fig. 5. Intensity of XRD by amorphous alloys: 1–$Co_{83}P_{17}$;2 – $Co_{85}P_{15}$; 3 – $Co_{90}P_{10}$.*Cu-Ka* radiation

Thus, determining the size of the regions of ordered scattering of atoms is necessary for further modeling of close-order amorphous and nanocrystalline alloys, and subsequently for specifying their physical parameters.

An analysis of literature data has shown that the radii of the first coordination (the smallest interatomic distances in amorphous Ni-P alloys) are in the range of 0.254—0.256 nm (in Fe-P alloys — 0.255—0.258 nm, and Co-P — 0.254—0.256 nm), while for crystalline б–Fe — 0.248 nm, , б–Co — 0.251 nm, , б–Co — 0.250 nm) [6—7]. In this regard, it is assumed that the close order of amorphous alloys has OVRAs with structures similar to the densest packings, forming lattices of the HCC, OCC, or HCC type. Similar structures are found in Ni, б–Fe, б–Co, б–Co metals and their phosphides (Ni_5P_2, $Ni_{2.55}P$, Ni_3P, $Ni_{12}P_5$, Fe_2P, Fe_3P, FeP_2, Co_2P, CoP_2, CoP_3, CoP_4, and others), which are formed during electrodeposition in the volume of amorphous Ni-P, Fe-P, Co-P alloys [8].

Diffractograms of $Ni_{86}P_{14}$, $Ni_{88}P_{12}$, $Ni_{90}P_{10}$, $Fe_{87}P_{13}$, $Fe_{85}P_{15}$, $Fe_{83}P_{17}$, $Co_{83}P_{17}$, $Co_{85}P_{15}$, $Co_{90}P_{10}$, alloys obtained in monochromatized Mo-Ka radiation and the structural factors calculated from them showed that they have different shapes, and therefore different structures, degrees of order, and vary depending on the chemical composition of the alloys (Figs. 6, 8, 10). The obtained diffractograms and structural factors made it possible to determine the following general patterns of close order of these

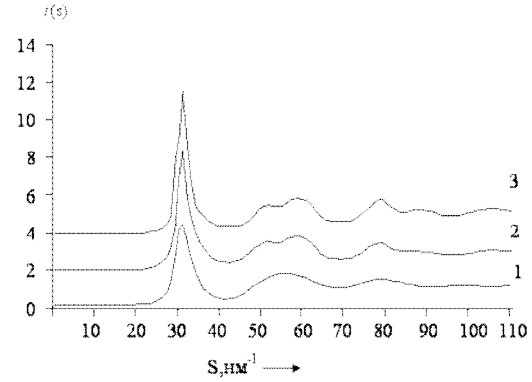

Fig. 6. Structural factors of amorphous alloys: 1 — $Ni_{86}P_{14}$, 2 — $Ni_{88}P_{12}$, 3 — $Ni_{90}P_{10}$

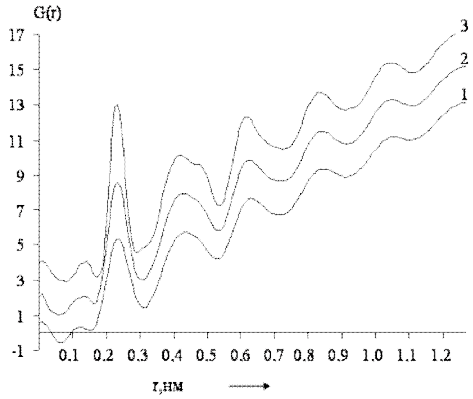

Fig. 7. FRRA of alloys 1 — $Ni_{86}P_{14}$, 2 — $Ni_{88}P_{12}$, 3 — $Ni_{90}P_{10}$

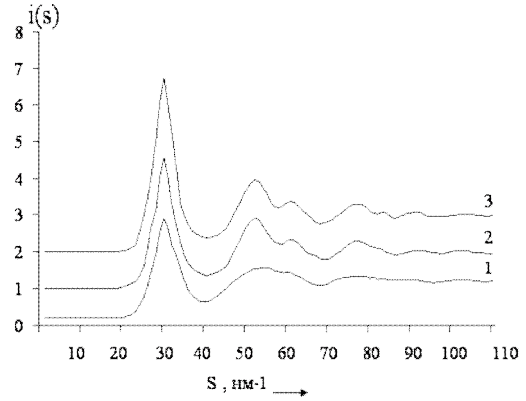

Fig. 8. Structural factors of amorphous alloys: 1 — $Fe_{83}P_{17}$, 2 — $Fe_{85}P_{15}$, 3 — $Fe_{87}P_{13}$

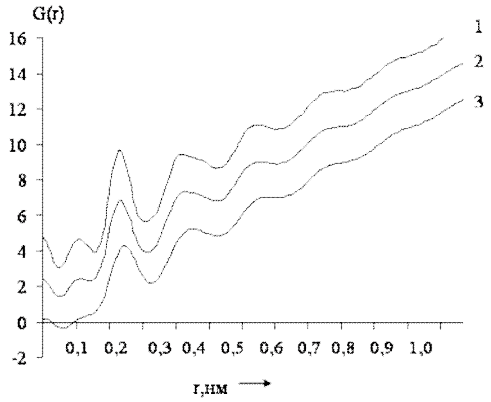

Fig. 9. FRRA of alloys:1 — $Fe_{83}P_{17}$, 2 — $Fe_{85}P_{15}$, 3 — $Fe_{87}P_{13}$

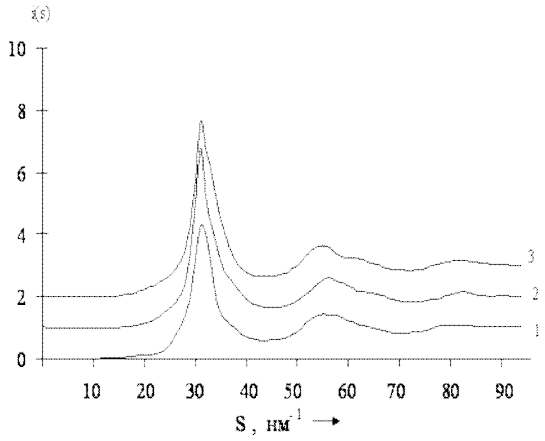

Fig. 10. Structural factors of amorphous alloys Co–P: 1 — $Co_{83}P_{17}$; 2 — $Co_{85}P_{15}$; 3 — $Co_{90}P_{10}$

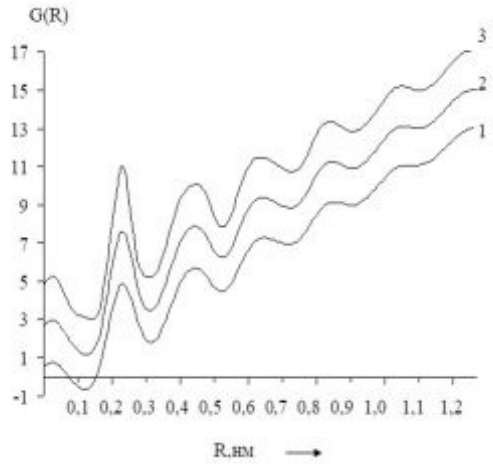

Fig. 11. FRRA of alloys Co–P: 1 — $Co_{83}P_{17}$; 2 — $Co_{85}P_{15}$; 3 — $Co_{90}P_{10}$

alloys. An increase in the prominence of the three diffuse peaks with a decrease in the phosphorus content indicates a restructuring of the amorphous phase towards its ordering, with the height of the first diffraction peak and its symmetry increasing, and its position shifting slightly towards higher values of S. Other peaks of the structural factor of Ni-P, Fe-P, and Co-P alloys have different shapes. For example, for N $Ni_{86}P_{14}$, the second maximum has a more symmetrical shape than for $Ni_{88}P_{12}$ and $Ni_{90}P_{10}$, where it is divided into two subpeaks, with the right subpeak being higher than the left. For $Fe_{83}P_{17}$ ($Co_{83}P_{17}$) alloys, the second maximum also has a more symmetrical shape than for $Fe_{85}P_{15}$ i $Fe_{87}P_{13}$ ($Co_{85}P_{15}$ and $Co_{90}P_{10}$) compositions, and for $Fe_{85}P_{15}$ and $Fe_{87}P_{13}$ ($Co_{85}P_{15}$ and $Co_{90}P_{10}$) compositions, it is divided into two subpeaks, with the left subpeak higher than the right. The change in the heights of the subpeaks of the second maxima depends on the amount of phosphorus and hydrogen that penetrate the lattice of the OVRA, which are associated with high values of overvoltage at the cathode [8]. With a decrease in the phosphorus content in alloys, the relief and peak heights increase (Fig. 6, 8, 10).

The study of the close order of amorphous alloys was carried out using its model and the FRRA approximation. According to the structural factors of amorphous alloys $Ni_{86}P_{14}$, $Ni_{88}P_{12}$ and $Ni_{90}P_{10}$, the functions of radial scattering of atoms of FRRA were calculated using formula (9) and the apodization coefficient ϕ=0,01, the graphs of which are presented in Fig. 9, curves 1—3 [2]. The FRRA curves were decoded by approximating them with a set of Gaussian peaks [2,6]. The symmetrical selection of XRD peaks showed that for Ni-P alloys the structure of the ordering regions is closest to the structure of the GCC of crystalline Ni, however, other types of structure similar to the OCC and the GCC are observed. Tabl. 1 shows the modeling data for the FRRA curves of $Ni_{86}P_{14}$, $Ni_{88}P_{12}$ and $Ni_{90}P_{10}$ alloys with an apodization coefficient of ϕ=0,01, the graphs of which are presented in Fig. 6 (curves 1—3, respectively). The modeling was performed by minimizing the radii of coordination spheres and coordination numbers of amorphous and crystalline structures. For the $Ni_{86}P_{14}$ alloy, the radii of coordination spheres with numbers 1, 2, 3, 4, 7, 9, 10 (Tabl. 1) coincided (with a slight error) with the radii of crystal spheres that describe the structure of the HCC and are close to the arrangement of atoms in crystalline Ni. For $Ni_{88}P_{12}$ and $Ni_{90}P_{10}$ alloys, the numbers of coordination spheres No1,2,3,4,7,9, 10 (Tabl. 1) and No1,2,3,4,7,9,10 (Tabl. 1) coincide. Coordination spheres No. 1, 2, 5, 6, 9, 10 (Tabl. 1) of $Ni_{86}P_{14}$ alloy are responsible for the location of inhomogeneities in Ni-P alloys by the type of CMC. For $Ni_{88}P_{12}$ and $Ni_{90}P_{10}$ alloys, the numbers of coordination spheres No. 1, 2, 6, 9, 10 (Tabl. 1) and No. 1, 2, 3, 4, 5, 6, 10 (Tabl. 1) coincide.

Table 1. Data on decoding the structure of Ni-P alloys by FRRA

	GCC, OCC*		$Ni_{86}P_{14}$			$Ni_{88}P_{12}$			$Ni_{90}P_{10}$		
№	(r_n/r_0)	Z	r_n	(r_n/r_0)	Z_n	r_n	(r_n/r_0)	Z_n	r_n	(r_n/r_0)	Z_n
1	1,000	12	2,448	1,00	10,318	2,438	1,000	10,251	2,426	1,000	12,014
1*	1,000	8	–	–	–	–	–	–	–	–	–
2*	1,155	6	3,00	1,227	0,385	2,896	1,189	1,256	–	–	–
2	1,414	6	3,451	1,409	3,305	3,578	1,467	4,12	3,300	1,358	0,925
3*	1,633	12	–	–	–	–	–	–	–	–	–
3	1,732	24	4,244	1,733	23,595	4,215	1,728	19,70	4,183	1,724	24,266
4*	1,914	24	–	–	–	–	–	–	–	–	–
4	2,000	12	5,025	2,053	18,061	4,956	2,0329	19,890	4,9811	2,053	19,119
5*	2,000	8	5,025	2,053	+	–	–	–	–	–	–
5	2,236	24	–	–	–	–	–	–	–	–	–
6*	2,309	6	5,745	2,348	12,204	5,692	2,335	9,416	5,7208	2,358	5,019
6	2,449	8	–	–	–	–	–	–	–	–	–
7*	2,516	24	–	–	–	–	–	–	–	–	–
8*	2,582	24	–	–	–	–	–	–	6,270	2,585	47,415
7	2,646	48	6,422	2,635	49,728	6,334	2,599	47,043	–	–	–
8	2,828	6	–	–	–	6,949	2,850	8,704	6,811	2,801	6,302

Continue of the table 1.

9*	2,828	24	–	–	–	6,949	2,850	–	–	–	–
9	3,000	36	7,347	3,001	34,621	7,310	2,998	30,458	7,273	2,998	35,249
10*	3,000	32	7,347	3,001	+	7,310	2,998	+	7,273	2,998	+
10	3,162	24	7,756	3,168	14,105	7,725	3,168	20,426	7,659	3,157	11,945

("+" means that the coordination spheres overlap)

The latter data relate to the forms that arise during the interaction between Ni and P atoms, since Ni and P compounds with different coordination polyhedra from cubic to trigonal can occur in the film volume. The volume fraction of OVRA with a structure similar to HCC with a decrease in the proportion of phosphorus from 14 to 10 % increases from 75 % for $Ni_{86}P_{14}$ to 91 % for $Ni_{90}P_{10}$. The OVRA structure of Fe-P alloys is close to that of HCC, but other types of structure are also observed. Tabl. 1 shows the data for decoding the FRRA curves of $Fe_{83}P_{17}$, $Fe_{85}P_{15}$ and $Fe_{83}P_{17}$ alloys calculated using formula (9) and the apodization coefficient ф=0,012, which are presented in (Fig. 9), respectively. The modeling was performed by comparing the radii of coordination spheres and coordination numbers of amorphous and crystalline structures.

Table 2. Data on the decoding of the structure of Co-P alloys by *FRPA*

	GCC, GCU* GCC**		$Co_{83}P_{17}$			$Co_{85}P_{15}$			$Co_{90}P_{10}$		
№	(r_n/r_0)	Z	r_n	(r_n/r_0)	Z_n	r_n	(r_n/r_0)	Z_n	r_n	(r_n/r_0)	Z_n
1	1,000	12	2,436	1,000	9,763	2,426	1,000	9,228	2,388	1,000	10,705
1*	1,000	8	2,436	1,000	+	2,426	1,000	+	2,388	1,000	+
2	1,414	6	3,118	1,280	3,102	–	–	–	–	–	–
2*	1,414	6	3,118	1,280	+	–	–	–	–	–	–
3*	1,633	12	–	–	–	–	–	–	–	–	–
4	1,732	24	4,206	1,727	22,318	4,186	1,725	22,821	4,117	1,724	20,393
5*	1,914	12	–	–	–	–	–	–	–	–	–
6	2,000	12	4,962	2,037	16,318	4.880	2.012	14.157	4,776	1,999	15,581
6*	2,000	6	4,962	2,037	+	4.800	2.012	+	4,776	1,999	+
7	2,236	24	5,526	2,268	8,696	–	–	–	–	–	–
7*	2,236	12	5,526	2,268	+	–	–	–	–	–	–
8	2,381	12	–	–	–	–	–	–	–	–	–
8	2,449	8	5,964	2,449	7,425	–	–	–	–	–	–
8*	2,449	6	5,964	2,449	+	–	–	–	–	–	–
9	2,516	12	–	–	–	–	–	–	–	–	–
10	2,646	48	6,420	2,635	43,466	6.413	2.644	46.697	6,302	2,638	45,422
10*	2,646	24	6,420	2,635	+	6,413	2,644	+	6,302	2,638	+

For the $Fe_{83}P_{17}$ alloy, the radii of the coordination spheres with numbers 1, 2, 3, 4, 7, 8, 9, 10 (Tabl. 2) coincide with a slight error with the crystal spheres that describe the structure of the OCC [9] and are close to the arrangement of atoms in crystalline б–Fe. For $Fe_{85}P_{15}$ and $Fe_{87}P_{13}$ alloys, the numbers of coordination spheres No. 1, 2, 3, 6, 7, 8, 9, 10 (Tabl. 2) and No. 1, 2, 3, 4, 7, 8, 9, 10 (Tabl. 2) coincide. Coordination spheres No. 1, 7, 9, 10 (Tabl. 2) of $Fe_{83}P_{17}$ alloy are responsible for the type of packing in the OVRA of Fe-P alloys by the type of OCC. The latter data relate to the forms that arise during the interaction between Fe and P atoms, since Fe-P compounds with different coordination polyhedra from cubic to trigonal can occur in the alloy volume. The deviation of the coordination distances and coordination numbers from those for the crystalline metal OCC can be explained by the fact that there are areas between the OVRA that are chaotically filled with phosphorus and hydrogen

atoms that do not form any strict structure and penetrate into the tetrahedral and octahedral pores. The volume fraction of OVRA with a structure similar to the OCC with a decrease in the proportion of phosphorus from 17 to 13 % increases from 71 % in $Fe_{83}P_{17}$ to 92 % for $Fe_{87}P_{13}$.

In Co-P alloys, the structure of the OVRA is closest to that of the HCC, but the types of the HCC and OCC structures are also observed. The data of modeling the FRRA curves of $Co_{83}P_{17}$, $Co_{85}P_{15}$ and $Co_{90}P_{10}$, alloys are given in Tabl. 2 and calculated using formula (9) and the apodization coefficient $\tau = 0.01$, which are presented in Fig. 11. For the $Co_{83}P_{17}$ alloy, the radii of coordination spheres with numbers 1, 2, 4, 6, 7, 8, 9, 10 (Tabl. 2) coincide with an error (≈2 %) with crystal spheres that describe the structure of the HCC [10] and are close to the way atoms are arranged in crystalline α-Co. For the $Co_{85}P_{15}$ and $Co_{90}P_{10}$ alloys, the numbers of coordination spheres are the same: 1,4,6,10,14,18,19,20 (Tabl. 2) and 1,4,6,7,9,10 (Tabl. 2).

Coordination spheres No. 1, 2, 6, 7, 8, 10 (Tabl. 2) of $Co_{83}P_{17}$ alloy are responsible for the arrangement of atoms in Co-P alloys by the type of HSC. Similarly, for Co85P15 and Co90P10 alloys, the numbers of coordination spheres No. 1, 6, 10 coincide (Tabl. 2). The latter data relate to the forms that arise during the interaction between Co and P atoms, since Co-P compounds with different coordination polyhedra from cubic to trigonal can occur in the alloy volume. The volume fraction of OVRA with a structure similar to HCC, with a decrease in the proportion of phosphorus from 17 to 10 at. % decreases from 86 % for $Co_{83}P_{17}$to 39 % for $Co_{90}P_{10}$, and the volume fraction of the structure similar to HCC increases from 3 to 48 %.

Conclusions

The conditions for obtaining reliable radial atom distribution function (RAF) curves were found. The concept of the *FRPA.* apodization coefficient for transition metal-metalloid systems was introduced to reduce the influence of the break in the experimental intensity curves. When integrating the experimental structural factor from 0 to the final value, which depends on the experimental conditions. The error that occurs during the experiment is minimized and the optimal apodization coefficient is determined

A close-order modeling of amorphous alloys Ni-P, Fe-P, Co-P was performed depending on the amount of metal. Small-angle studies were used to determine the average size of coherent scattering regions.

Close-order modeling has shown that with a decrease in the amount of phosphorus, the relief and peak heights increase, the difference in coordination numbers of amorphous alloys from similar crystalline transition metals is explained by the presence of a highly disordered close order and gaps that do not have ordered formations. The modeling allowed us to establish that the probability of formation of close-order alloys in the structure is associated with non-equilibrium deposition conditions, in particular, with a high value of overvoltage at the cathode and penetration of phosphorus atoms into the structure of alloys.

References

[1] Baskevich, O.S. (2008). Formuvannya amorfnih splaviv perehidnih metaliv z fosforom pri elektroimpulsnomu osadzhenni [Formation of amorphous transition metal-phosphorus alloys by electroimpulse deposition]. (Diss. Ph.D. physics and mathematics of science), Dnipropetrovsk National University of Railway Transport named after V. Lazaryan.

[2] Hulivets, A.N., Baskevich, A.S., & Shtapenko, E.F. (2001). Izuchenie lokalnoj atomnoj struktury amorfnyh splavov Co–P i Ni–P [Study of the local atomic structure of Co–P and Ni–P amorphous alloys]. *Visnyk Dnipropetrovskoho Natsionalnoho Universytetu*, Ser. Physics. Radioelectronics, 7, 3–8.

[3] Baskevich, O.S., Hulivetz, A.N., & Zabludovsky, V.O. (2004). Modelirovanie blizhnedejstvuyushih struktur v splavah Ni–P [Modeling of short-range structure in Ni–P alloys]. *Ukrainian Journal of Physics*, 49(12), 1196–1199.

[4] Hulivets, A.N., Baskevich, A.S., & Shtapenko, E.F. (2000). Modelirovanie struktury amorfnyh plenok Co–P. [Modeling of the structure of Co–P amorphous membrans]. *Visnyk Dnipropetrovskoho Natsionalnoho Universytetu*, 6, 9–14.

[5] Baskevich, A.S., Hulivets, A.N., & Shtapenko, E.F. (2001). Lokalnaya atomnaya struktura amorfnyh plenok Co–P i Ni–P [Local atomic structure of Co–P and Ni–P amorphous membranes]. *8th International Conference on Physics and Technology of Thin membrans*, 174–175.
[6] Hulivets, A.N., Baskievich, A.S. (2017). Modelirovanie blizhnego poryadka amorfnyh splavov metall–metalloid [Modeling short-range order in amorphous metal-metalloid alloys]. *Mathematical Modeling*, 36(1), 78-80.
[7] Zabludovsky, V.A., Anishchenko, T.I., Gulivets, A.N., & Shtapenko, E.F. (2003). Vliyanie impulsnogo elektroliza na korrozionnuyu stojkost plenok [Influence of pulse electrolysis on the corrosion resistance of Co–P, Fe–P, Fe–Ni–P]. *In Proceedings of the 3rd International Scientific and Technical Conference "Surface Engineering and Renovation of Products*, 65-66.
[8] Baskevich, A.S., Gulivets, A.N., & Zabludovsky, V.A. (2004). Blizhnij poryadok rentgenoamorfnyh splavov Ni–P i Co–P, poluchennyh impulsnym elektroosazhdenie [Short-range order of X-ray amorphous Ni–P and Co–P alloys obtained by pulse electro-deposition]. *Metallofizika i Noveishie Tekhnologii*, 26(9), 1151-1161.
[9] Baskevich, A.S., Gulivets, A.N., Zabludovsky, V.A., & Kraeva, V.S. (2004). Izuchenie blizhnego poryadka rentgenoamorfnyh splavov Fe–P, poluchennyh elektroimpulsnym osazhdeniem [Study of the short-range order of X-ray amorphous Fe–P alloys obtained by pulse electro-deposition]. *Visnik Dnipropetrovskogo Natsionalnogo Universitetu.*, 12, 109-116.
[10] Danilov, F.I., Protsenko, V.S., Gordienko, V.O., Baskevich, A.S., & Artemchuk, V.V. (2012). Osazhdenie nanokristallicheskih hrom–uglerodnyh splavov iz elektrolita na osnove sulfata trehvalentnogo hroma s ispolzovaniem impulsnogo toka [Deposition of nanocrystalline chromium–carbon alloys from an electrolyte based on trivalent chromium sulfate using pulse current]. *Physicochemical of Surface and Protection of Materials*, 48(3), 280-285.

Список використаної літератури

1. Баскевич О.С. Формування аморфних сплавів перехідних металів з фосфором при електроімпульсному осадженні: дис. … канд. фіз..-мат. наук: 01.04.07; Дніпропетр. нац. ун-т залізн.. трансп. ім. В. Лазаряна. – Д., 2008. – 146 арк.
2. Гуливец А.Н. Изучение локальной атомной структуры аморфных сплавов Co–P и Ni–P / А.Н. Гуливец, А.С. Баскевич, Э.Ф. Штапенко. *Вісник Дніпропетровського національного університету*, Фізика. Радіоелектроніка. Дніпро. 2001. №.7. С. 3–8.
3. Baskevich O.S., Gulivetz A.N., Zabludovsky V.O. Modeling of short–range structure in Ni–P alloys. *Ukr. J. Phys*. 2004. V.49, №12. P. 1196–1199.
4. Гуливец А.Н. Баскевич А.С., Штапенко Э.Ф. Моделирование структуры аморфных пленок Co–P. *Вісник Дніпропетровського національного університету*. Сер.Фізика. Радіоелектроніка. Дніпро. 2000. №. 6. С. 9–14.
5. Баскевич А.С., Гуливец А.Н., Штапенко Э.Ф. Локальная атомная структура аморфных пленок Co–P и Ni–P. *8 Міжнародна конференція з фізики і технології тонких плівок*. Івано–Франківськ. 2001. С. 174–175.
6. Гуливец А.Н., Баскевич А.С. Моделирование ближнего порядка аморфных сплавов металл–металлоид. *Математичне моделювання*. 2017. Т.36, №1. С.78–80.
7. Заблудовский В.А. Анищенко Т.И., Гуливец А.Н., Штапенко Э.Ф. Влияние импульсного электролиза на коррозионную стойкость пленок Co–P, Fe–P, Fe–Ni–P . *Материалы 3–й Международной научно–технической конференции «Инженерия поверхности и реновация изделий»*. Киев. 2003. С. 65–66.
8. Баскевич А.С. Гуливец А.Н, Заблудовский В.А. Ближний порядок рентгеноаморфных сплавов Ni–P и Co–P, полученных импульсным электроосаждение. *Металлофизика и новейшие технологии*. 2004. Т. 26, № 9. С. 1151–1161.
9. Баскевич А.С. Гуливец А.Н., Заблудовский В.А., Краева В.С. Изучение ближнего порядка рентгеноаморфных сплавов Fe–P, полученных електроимпульсным осаждением. *Вісник Дніпропетровського національного університету*. Дніпро. 2004. №.12. С. 109–116.

10. Данилов Ф.И., Проценко В.С., Гордиенко В.О., Баскевич А.С., Артемчук В.В. Осаждение нанокристаллических хром–углеродных сплавов из электролита на основе сульфата трехвалентного хрома с использованием импульсного тока. *Физикохимия поверхности и защита материалов*. 2012. Т.48, №3. С.280–285.

Надійшла до редколегії 04.07.2023